Assembly of microspheres with polymers by evaporating emulsion droplets

Keng-hui Lin,[1,2,4] Liang-jie Lai,[1] Chih-Chung Chang,[2] and Hui Chen[2]
[1]*Department of Physics, National Central University, Chungli, Taiwan 320*
[2]*Department of Chemical and Materials Engineering, National Central University, Chungli, Taiwan 320*
[3]*Institute of Physics, Academia Sinica, Taipei, Taiwan 115*
[4]*Research Center for Applied Sciences, Academia Sinica, Taipei, Taiwan 115*
(Received 18 August 2008; published 28 October 2008)

We study the packing of colloidal microspheres mixed with polymers in oil-in-water emulsion droplets by evaporation. The addition of polymers produces non-unique configurations of final clusters when the number of particles N inside the droplet is larger than 4. The cluster configurations are classified into three categories based on symmetry. Stablized colloidal clusters of spherical packings are observed. Our observations on packing process suggest the mechanisms which cause different and nonunique structures. The osmotic pressure and the interparticle interaction due to polymers changes the force balance between microspheres and result in different structures.

DOI: 10.1103/PhysRevE.78.041408 PACS number(s): 82.70.Dd, 61.30.Hn, 61.46.Bc, 68.05.−n

The assembly of colloidal particles into novel structures has always been an attractive challenge for material scientists [1,2]. Nonspherical, anisotropic colloidal particles or "colloidal molecules" open up the possibilities for non-close-packed structures such as a diamond structure [3]. This potentially provides a paradigm for the creation of three-dimensional photonic structures [4]. Understanding the rules of assembly may shed light on the intricate assembly of biological systems such as viruses. It is also interesting to note that colloidal assembly is connected to optimal packing problems in mathematics. For example, the mean-field calculation implies thermodynamically stable hard sphere structures in infinite space have the most effecient packing (Kepler conjecture) though some more detailed theoretical calculation and experimental observation shows minute differences in entropy between face centered cubic and hexagonal close packed structures. The mathematical work on packing problems may provide insights on studying the assembly of colloidal microspheres [5].

One intriguing class of packing problems is spherical packings. Different optimization conditions yield to different symmetries and packings [6]. Many of the spherical packing problems have been inspired by observing the nature. When the biologist Tammes observed the arrangement of pores on pollen grains in 1930, he posed the question, "Given a minimal distance between points, how many points N can be put on the sphere? What is the arrangement? Is it unique?." This is still an unsolved question in geometry. The solutions up to $N=130$ is available on Sloane's website [7]. Part of our colloidal clusters exhibit the structures of the solutions to the Tammes problem.

Recently Manoharan, Elsesser, and Pine invented a simple method to make colloidal clusters. They observed the packing of hard-sphere-like microspheres in oil-water emulsion droplets. The microspheres attached to the interface of emulsion droplets and oil was subsequently removed from the emulsion droplets, leaving the microspheres in compact clusters. The final particle packings were unique for $N \leqslant 15$ and the observed packings for $N \leqslant 11$ followed minimal second moment particle distribution $\mathcal{M}=\Sigma_{i=1}^{N}|\mathbf{r}_i-\mathbf{r}_0|^2$ where $\mathbf{r}_i$ is the center of the ith sphere and $\mathbf{r}_0$ is the center of mass of the cluster [8]. Lauga and Brenner later explained the unique assembly as depicted in Figs. 1(a)–1(c). The process included (i) the microspheres being bound to 2D droplet surfaces and (ii) the uniqueness of initial spherical packing of the particles at the critical volume where the microspheres in contact with one another and the interface of droplets started

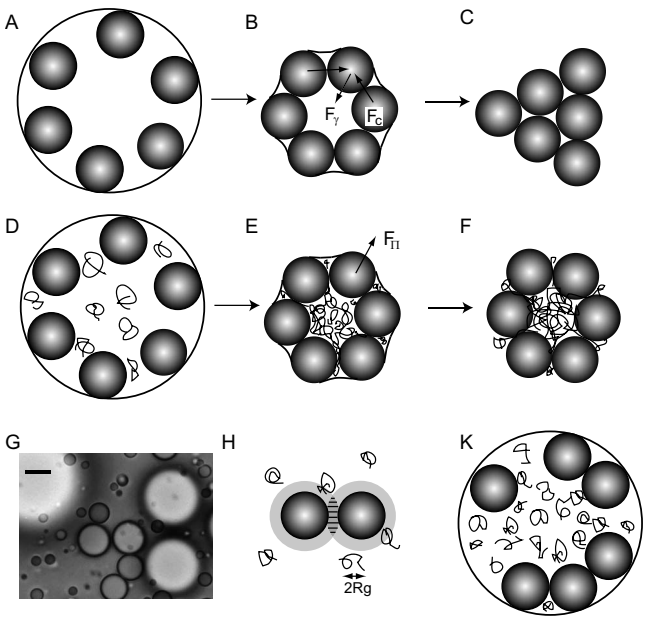

FIG. 1. The schematics of two-dimensional representation of the drying process: (A) microsphere configuration above the critical volume, (B) At critical packing there is a balance between the capillary force F_γ and the contact force F_c from the nearby particles, (C) final packing with polymer stabilized inside. The schematics of the drying process with polymers inside: (D) microsphere or polymer in an emulsion droplet, (E) osmotic force F_Π exerted by the polymers, (F) final packing. (G) Initial polydisperse droplets. The scale bar is 10 μm. (H) Polymer depletion in the dilute regime. The depletion region is shaded in grey and the hatched region corresponds to the overlapped depletion zone. (K) The depletion doublets and triplets formed inside an emulsion droplet.

to deform. The capillary force F_γ collapsed the initial spherical packing in the highly constrained condition. The final minimal second moment structures are a result of force balance between F_γ and the contact force F_c from the neighboring microspheres [9]. Lauga's theory and Manoharan's observation both show the importance of the intermediate stage of spherical packings during the assembly process. Since then, there have been many other works, both theoretically and experimentally, that have investigated assembling clusters with spherical symmetry [10–15].

In our experimental systems, we added polymers into emulsion droplets [Fig. 1(d)]. What roles does polymer possibly play in the process of packing? First, polymer coils exert the osmotic pressure inside emulsion droplets [Fig. 1(e)]. Osmotic pressure Π becomes significant at the semidilute region and is given by [16]

$$\Pi = \frac{\rho RT}{M}\left(\frac{\rho}{\rho^*}\right)^{5/4} \text{(semidilute)}, \tag{1}$$

where R is the ideal gas constant, T is the temperature, M is the molecular weight, ρ is polymer concentration, and ρ^* is the polymer critical concentration. The critical concentration ρ^* was calculated as 26 mg/ml. The estimated oil-water interfacial tension γ in the presence of Pluoric triblock surfactant was around 20 mN/m [17] which gives rise to the Laplace pressure 40 kPa of an emulsion droplet of 1 μm in radius. When the concentration of polymer inside the emulsion reached 154 mg/ml by more than a fivefold decrease in radius, the osmotic pressure due to the polymer was equal to 40 kPa. An extra osmotic force F_Π outward in addition to F_γ and F_c is involved in the particle rearragement shown in Figs. 1(d) and 1(e). As shown in Fig. 1(g), our initial emulsion droplets are polydisperse and could be as large as 10 μm in radius. The osmotic force in an evaporated droplet was strong enough to overcome the capillary force.

In addition to the interaction between the microspheres and the interface, the polymers also modified the interaction between microspheres by inducing depletion attraction as illustrated in Fig. 1(h). A particle immersed in a polymer solution experiences an osmotic pressure acting normal to its surface. At dilute concentration, polymer can be modeled as an ideal gas of hard spheres with the size of radius of gyration R_g of the polymer coils. Polymer coils are depleted within a layer of thickness R_g near the microsphere surface because the centers of the polymer "sphere" are excluded from the depletion region. When depletion layers of two microspheres are overlapped, the polymer is excluded from the overlapped depletion zone. As a result, the pressure due to the polymer solution is unbalanced, resulting in an attraction. The attractive potential between microspheres can be calculated as the work done by polymer coils. The potential depth at contact is $U_0 \approx -2\pi a R_g^2 n k_B T$, where a is sphere radius, n is the number density of polymer, k_B is Boltzmann's constant, and T is temperature [18]. When the polymer concentration is increased above the critical concentration ρ^*, the polymer is characterized by a correlation length ξ rather than by R_g. A depletion attraction still occurs and the length scale becomes ξ [19]. In our system, there was no repulsive interaction due to polymer adsorption which is confirmed by the bulk experiment—colloidal microspheres all flocculated or crystallized as the polymer concentration ranged from 1 to 20 mg/ml. Due to depletion attraction, microspheres may have formed doublets, triplets, or small 2D crystallites on the droplets surface. The initial packing and the force balance conditions changed at critical volume. The final packing deviates from the initial packing condition where all microspheres are freely moving. In our experiment, R_g was about 11 nm [20] and the polymers at the initial concentration induced 2.6–4.4 k_BT pairwise depletion attraction between microspheres.

Our samples were prepared by mixing 1% homemade monodisperse crosslinked polystyrene/divinylbenzene (PS/DVB) microspheres of 1 μm in diameter with polystyrene (PS) polymer of 88,000 dalton (Fluka, $M_w/M_n=1.08$) both in toluene [21]. The mixture was then dispersed in 1% w/w Pluronic F108 surfactant aqueous phase and emulsified with a homogenizer (IKA model T25) at 11,000 rpm for one minute. After homogenization, the emulsion was diluted with deionized water and heated at 100 °C for a few hours or left overnight at room temperature to allow the toluene to evaporate. After the toluene had completely evaporated, clusters of different sizes were left in the suspension. Each cluster was formed in a single emulsion droplet containing various amounts of spheres and polymers due to the initial polydisperse droplets. Clusters of different sizes are roughly fractionated by density gradient centrifiguration [8]. Some PS/DVB particles show slight deformation under the scanning electron microscope (SEM). This has little effect on the results. The particles maintain spherical in toluene. In the control experiment with PS polymer added, the results are identical to Manoharan's result.

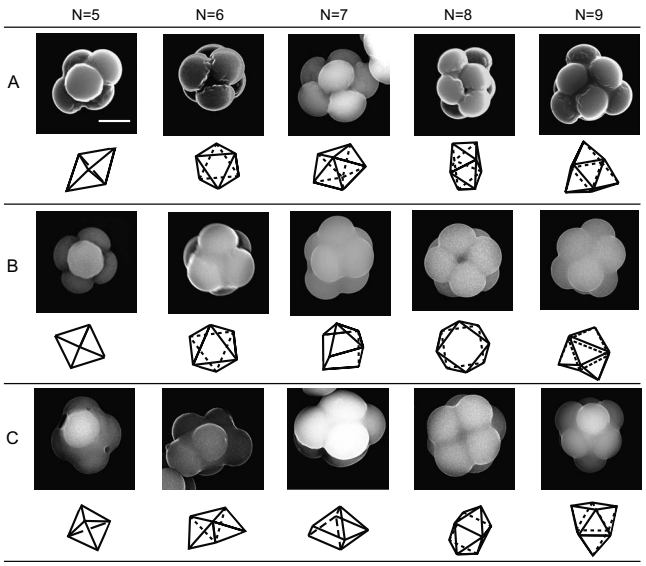

FIG. 2. Cluster configurations for $N=5-9$. The scale bar is 1 μm. The images were digitally processed to reduce background noise and increase contrast. The top rows show the electron micrographs of the clusters and the bottom rows illustrate the polyhedra by treating the center of the sphere as a vertex. The clusters in row A satisfy minimal second moment distribution. The clusters in row B agree with solutions to the Tammes problem. The clusters in row C do not belong to A and B.

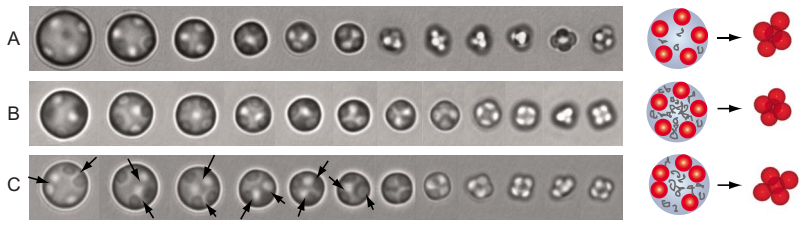

FIG. 3. (Color online) Optical micrographs of the packing process for category A, B, and C. The cartoons in the right column show possible starting conditions for each category. The arrows in row C point two doublets in the emulsion droplet. They never come apart thoughout the packing process. Movies are available as auxiliary materials [23].

Clusters of unique configurations are only observed when $N \leqslant 4$, i.e., a linear doublet ($N=2$), a triangular trimer ($N=3$), and a tetrahedral tetramer ($N=4$). When $N>4$, there are more than one final configurations for each N. Figure 2 shows the configurations for $N=5-9$. In the following discussion, cluster configurations are referred as polyhedra by treating each sphere center as a vertex. The configurations are classified into three categories. The first category A consists of clusters which minimize the second moment of mass distribution [Fig. 2(a)]. The second category B consists of clusters which satisfy the solutions to the Tammes problem [Fig. 2(b)]. This is confirmed by drawing 3D polyhedra based on the coordinates from [7] and by comparing cluster SEM images against the 2D projection of polyhedra of spherical packings. The third category C consists of the clusters which do not belong to category A and B [Fig. 2(c)]. Polymer concentration is an important factor for different category population. Triangular dipyramids are more often found at lower initial polymer concentrations. At 1 mg/ml PS, triangular dipyramids account for 75% in $N=5$ cases. At 1.7 mg/ml PS, the percentage drops to below 50%.

We observed the evaporation processes of droplets containing $N=5$ to illustrate routes to different structures. Figure 3 shows time-lapse frames of scenarios A, B, and C corresponding to clusters of categories A, B, and C, respectively. The particles were all initially bound to the droplet interface. Before the droplet was deformed, microsphere movement in scenarios A and B were similar. They are freely diffusing at the interface of the droplet. In scenario A, the microspheres were arranged as spherical packings at the critical volume. They appeared in contact with each other and showed no relative motion to one another. The interface deformed rapidly and the capillary force from the deformed interface pushed microspheres inward and was balanced by the contact force between microspheres. The microspheres were collapsed into minimal second moment distributions. In scenario B, the microspheres were arranged as spherical packings at the critical volume as well. The droplet evaporated more slowly in comparison with scenario A. The optical image of microspheres in a droplet generally showed less contrast and blurred boundary from the higher concentration of polymer in the background oil. The viscosity also increased and might accounted for the kinetic stability of microspheres to move separately as individuals. The final packing of microspheres remained spherical packings. The polymer inside emulsion droplets exerted high enough osmotic pressure to balance the capillary force which drew particles toward inside. Therefore, microspheres became "stablized" as the spherical packing structures instead of collapsing into the minimal second moment structures.

The process that was undertaken to form configurations of category C is not unique and even explains the multiple configurations in this category. Due to the polymer depletion interaction, microspheres formed doublets, triplets, or 2D crystallites on the interface before the droplets deform. Figure 3(c) shows that two pairs of doublets and one singlet in an emulsion droplet. Through the shrinking stage, the doublets never separated. This changed the initial packing of particles on the spherical droplet surface before rearrangement. On some occasions we observe 3D colloidal clusters inside emulsion droplets. In this case, Lennard-Jones clusters may have be formed [22]. This situation was largely observed for large N.

To summarize, the addition of polymer changed the force balance in microsphere rearrangement and resulted in multiple configurations when $N>4$. When colloidal microspheres initially are free to move as individuals at the droplet surface, microspheres are packed into spherical packings at the critical volume. In the case of no or low polymers, the spherical packing at the critical volume was collapsed into the minimal second moment configuration. At high enough concentration of polymers, the spherical packing structure at the critical volume was stabilized even when the oil completely evaporated. The depletion attraction between the colloidal particles changed the the initial spherical packing at the critical volume. Thus, the force balance between different microsphere was altered and resulted in many variations. Our work is in agreement with the observations of patched supraparticles by Cho *et al.* [15,20]. In Cho's work [15] bidisperse colloidal microspheres were mixed in the emulsion droplets. Two configurations for $N=8$ were reported—one was square antiprism (the spherical packing) and the other was snub disphenoid (the minimal second moment). In Ref. [20], where the PS homopolymer ($M_w=9100$ Dalton) was added to the emulsion droplets, multiple motifs for $N>4$ were reported. Our work categorizes the multiple configurations, illustrates possible mechanisms and supports the theory by Brenner and Lauga.

We thank P-Y. Lai and John C. Crocker for helpful discussion and we also thank Wuen-shiu Chen and Yun-ting Chen for help with experiments. Support for this work was provided by NSC Grant No. 96-2112-M-001, the starting fund from Institute of Physics and the nanobio program of the Research Center for Applied Sciences, Academia Sinica.

[1] Y. Yin, Y. Lu, B. Gates, and Y. Xia, J. Am. Chem. Soc. **123**, 8718 (2001).
[2] A. van Blaaderen, Science **301**, 470 (2003).
[3] Z. L. Zhang, A. S. Keys, T. Chen, and S. C. Glotzer, Langmuir **21**, 11 547 (2005).
[4] K. M. Ho, C. T. Chan, and C. M. Soukoulis, Phys. Rev. Lett. **65**, 3152 (1990).
[5] S.-H. Mau, Ph.D. Thesis, Princeton University, Princeton, 2000.
[6] T. Aste and D. Weaire, *The Pursuit of Perfect Packing* (Institute of Physics Publishing, Bristol, 2000).
[7] N. J. A. Sloane, with the collaboration of R. H. Hardin and W. D. Smith and others, Tables of Spherical Codes, published electronically at http://www.research.att.com/~njas/packings/
[8] V. N. Manoharan, M. T. Elsesser, and D. J. Pine, Science **301**, 483 (2003).
[9] E. Lauga and M. P. Brenner, Phys. Rev. Lett. **93**, 238301 (2004).
[10] T. Chen, Z. Zhang, and S. C. Glotzer, Proc. Natl. Acad. Sci. U.S.A. **104**, 717 (2007).
[11] J.-R. Roan, Phys. Rev. Lett. **96**, 248301 (2006).
[12] M. Schnall-Levin, E. Lauga, and M. P. Brenner, Langmuir **22**, 4547 (2006).
[13] L. Hong, A. Cacciuto, E. Luijten, and S. Granick, Nano Lett. **6**, 2510 (2006).
[14] G. R. Yi *et al.*, Adv. Mater. (Weinheim, Ger.) **16**, 1204 (2004); S.-H. Kim *et al.*, J. Am. Chem. Soc. **128**, 10897 (2006).
[15] Y.-S. Cho *et al.*, J. Am. Chem. Soc. **127**, 15968 (2005).
[16] M. Doi and S. F. Edward, *The Theory of Polymer Dynamics* (Oxford Science Publications, Oxford, 2001).
[17] T. F. Svitova and C. J. Radke, IEEE J. Sel. Top. Quantum Electron. **44**, 1129 (2005).
[18] A. Vrij, Pure Appl. Chem. **48**, 471 (1976).
[19] R. Verma, J. C. Crocker, T. C. Lubensky, and A. G. Yodh, Phys. Rev. Lett. **81**, 4004 (1998).
[20] Y.-S. Cho *et al.*, Chem. Mater. **19**, 3183 (2007).
[21] J.-L. Ou, M.-H. Wu, and H. Chen, J. Mater. Sci. Lett. **20**, 2221 (2001).
[22] M. R. Hoare and J. McInnes, Faraday Discuss. Chem. Soc. **61**, 12 (1976).
[23] See EPAPS Document No. E-PLEEE8-78-195810 for movies of the packing process. For more information on EPAPS, see http://www.aip.org/pubservs/epaps.html.